Draft version January 19, 2016
Preprint typeset using LaTeX style emulateapj v. 12/16/11

AXISYMMETRIC DYNAMICAL MODELLING IN THE PRESENCE OF SPIRAL ARMS IN THE MILKY WAY DISK

Wilma H. Trick[1,2], Jo Bovy[3], and Hans-Walter Rix[1]

Draft version January 19, 2016

ABSTRACT

We are going to apply RoadMapping - an axisymmetric action-based dynamical modelling approach using smooth distribution functions (DFs) for Galaxy disk stars to recover the gravitational potential (Trick, Bovy, & Rix 2016, submitted) - to the positions and velocities of star particles from a simulation snap-shot of a MW-like disk galaxy (D'Onghia et al.) with pronounced non-axisymmetries like spiral arms. We expect to find that for small survey volumes, in which one spiral arm strongly dominates the observed dynamics, our smooth model fails to recover the true potential. For large enough survey volumes that encompass more than just a few spiral arms, we hope however that their effect on the dynamics averages out and we are able to constrain the true potential to within 10Because the simulation has no information about stellar chemical abundances, we treat the whole disk as a single stellar population. It would be very encouraging if we found that in this case fitting a superposition of only two quasi-isothermal DFs already allows for enough freedom to find a smooth equilibrium model for the entire disk. The use of more components or more complex, physically-motivated DFs could only seem justified, if we also explicitely treat spiral arms in the DF. We would like to propose a very simple outlier model for spiral arms, that can be included in the modelling to guide the fit towards a realistic Galaxy equilibrium model. It would be great if we could also show how such an equilibrium model helps to identify substructure in the disk. And last but not least, we would like to present a numerical method in the appendix, that helps to calculate the smooth density distribution of a given DF and potential to high numerical accuracy efficiently and with much less computational cost than in previous implementations of RoadMapping. In addition we ague, that fitting a Stckel potential directly to the data instead of using a physically-motivated galaxy potential has some advantages: Firstly, this is computationally *much* faster and secondly, the introduced error in the Action calculation is of similar or smaller size than other non-convergent Action calculation methods (see Sanders & Binney 2015). This makes RoadMapping finally fit to be applied to real data.

Keywords: Galaxy: disk — Galaxy: fundamental parameters — Galaxy: kinematics and dynamics — Galaxy: structure

1. THE SIMULATION

1.1. *General information*

- *Snapshot name:* snap_005
- *Snapshot time:* 250 Myr
- *Reference:* D'Onghia et al. (2013) [TO DO: I'm not sure...]

1.2. *Particle Types*

- *Particle Type 2: Disk stars.* 100 Million particles. Mean mass: $\sim 370 M_\odot$.
- *Particle Type 3: Bulge stars.* 10 Million particles. Mean mass: $\sim 950 M_\odot$.
- *Particle Type 4: Giant Molecular clouds / perturbers.* 1000 particles. Mean mass: $9.5 \cdot 10^5 M_\odot$. Distributed in thin disk. (D'Onghia et al. 2013)

[1] Max-Planck-Institut für Astronomie, Königstuhl 17, D-69117 Heidelberg, Germany
[2] Correspondence should be addressed to trick@mpia.de.
[3] Department of Astronomy and Astrophysics, University of Toronto, 50 St. George Street, Toronto, ON, M5S 3H4, Canada

1.3. *Coordinate System*

Calculate moment of intertia (in % units of largest entry):

- Star particles type 2, origin = $(0,0,0)$ (used in analysis for simplificity):

$$\bar{\bar{I}} = \begin{pmatrix} 50.1027 & 0.1950 & -0.0074 \\ 0.1950 & 50.2274 & -0.0044 \\ -0.0074 & -0.0044 & 100 \end{pmatrix}$$

- Star particles type 2, origin = $(-0.007, 0.002, -0.001)$ (particle position with deepest potential):

$$\bar{\bar{I}} = \begin{pmatrix} 50.1027 & 0.1950 & -0.0074 \\ 0.195 & 50.2273 & -0.0044 \\ -0.0074 & -0.0044 & 100 \end{pmatrix}$$

- Particles type 2, 3 and 4, origin = $(-0.008, 0.004, -0.003)$ (particle position with deepest potential):

$$\bar{\bar{I}} = \begin{pmatrix} 88.598 & 0.090 & 0.015 \\ 0.090 & 89.225 & 0.467 \\ 0.015 & 0.467 & 100 \end{pmatrix}$$

- I think I can safely assume that the origin of the static halo is at (0,0,0).

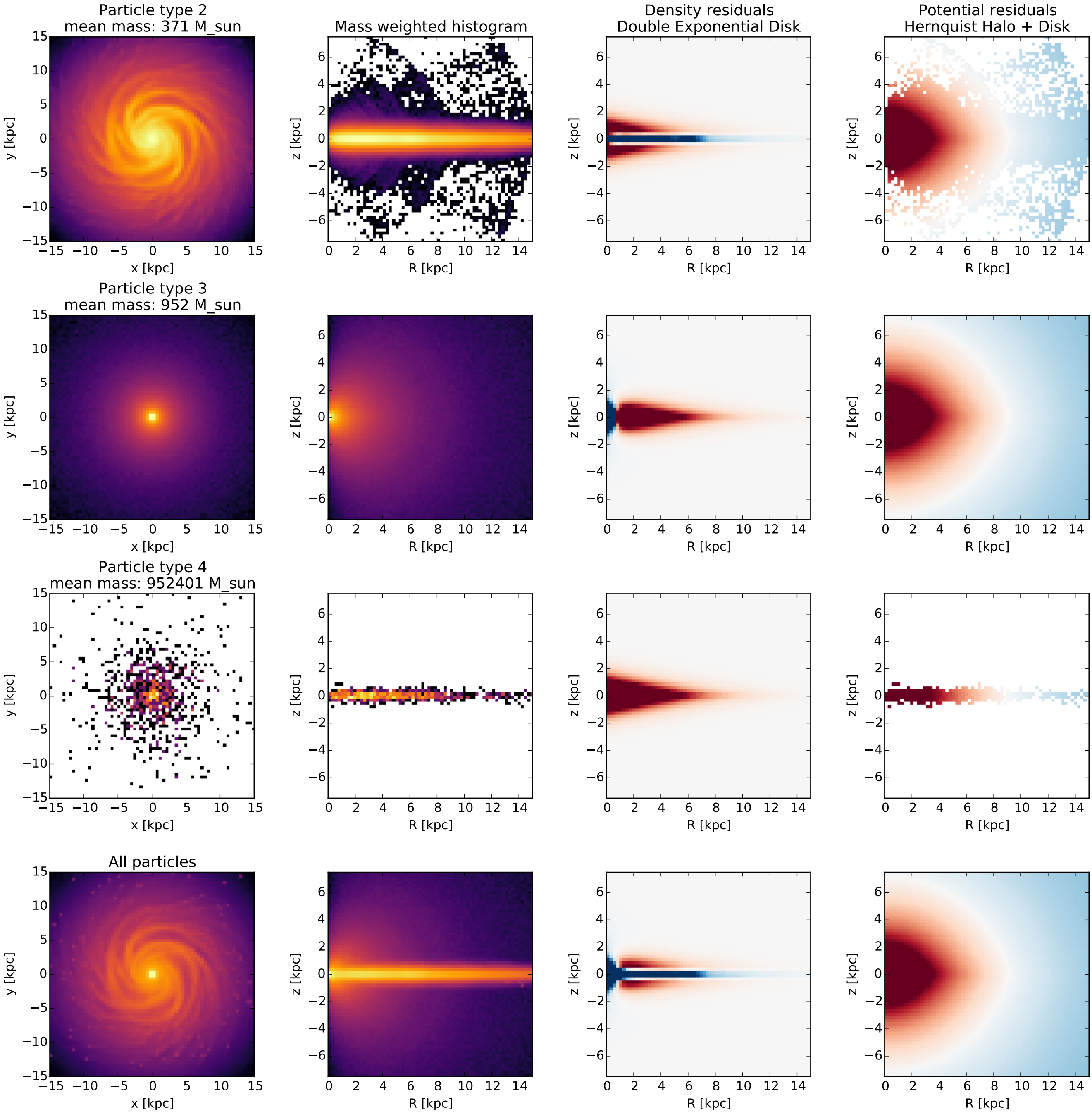

Figure 1. First two columns: Mass-weighted histograms of the 3 particle types. Third column: Density residuals between particle density of type x and a double exponential disk with $h_R = 2.5$ kpc and $h_z = 0.1h_R$ and $M_{\mathrm{disk}}/M_{\mathrm{halo}} = 0.04$. According to D'Onghia et al. (2013); Springel et al. (2005) this is actually supposed to be a disk with $\rho(R,z) = \frac{M_{\mathrm{disk}}}{4\pi h_z h_R^2} \operatorname{sech}^2(z/h_z) \exp(-R/h_R)$. Fourth column OBSOLETE!: Potential residuals between average potential keyword POT per bin and potential generated by the exponential disk and an Hernquist halo with $M_{\mathrm{halo}} = 9.5 \cdot 10^{11} M_\odot$ and a scale length of 160 kpc. What is actually going on here: Keyword POT is the potential of the particles only. The dark matter halo has a scale length of 29 kpc. So the plots in this fourth column doesn't make sense at all.

1.4. *Disk Scale Length*

I fitted an radially exponential profile to the azimuthally averaged surface density of the star particles (2). I found

$$R_s = 2.4993$$

As the Milky Way's disk scale length is also approximately 2.5 kpc, I can use the galaxy as it is. Lengths are in units of kpc, velocities in km/s, masses in $10^{10} M_\odot$. According to the read-me file, the scale length is also 2.5 kpc.

1.5. *Analytic Dark Matter Halo*

The dark matter halo is static and has a Hernquist profile.

- $M_{halo} = 95 \cdot 10^{10} M_\odot$. (D'Onghia et al. 2013) (Email by Elena D'Onghia on 3. Aug 2011)
- Hernquist scale length: 29 kpc according to Email by Stephen Pardy on 8. January 2016
- Email by Elena D'Onghia on 3. Aug 2011: "[...] an Hernquist halo with total mass of $9.5 \cdot 10^{11}$ Msun computed at a radius of 160 kpc. The halo is simulated with a rigid potential. The concentration of the halo is adopted to be c=9 for an HErnquist profile qhich is approximately like c=12 for a NFW profile. [...]"
- [TO DO: I have no way to cross check the validity of the information on the scale length a that they gave me. Is the info from 2016 and 2011 consistent with each other? What is the concentration of a Hernquist halo?]

1.6. *Bulge*

According to Springel et al. (2005) the bulge has a Hernquist profile. And according to the email from 3. Aug 2011 the scale length is 0.1 * disk scale length. From fitting a Hernquist potential I get $a = 0.25099812$ kpc.

[TO DO: According to the Email from 3. August 2011 the total disk mass is $0.04 \cdot 95 \cdot 10^10 M_\odot = \cdot 10^10 M_\odot$. By summing up all particles of type 2 and 4 I get: $3.80960311511 \cdot 10^10 M_\odot$. Similar for the bulge: they claim $0.01 \cdot 95 \cdot 10^10 M_\odot$ but I measure $0.952400755715 \cdot 10^10 M_\odot$.]

1.7. *Disk*

The disk is supposed to have a profile:

$$\rho(R, z) = \frac{M_{\text{disk}}}{4\pi h_z h_R^2} \operatorname{sech}^2(z/h_z) \exp(-R/h_R)$$

with $h_R = 2.5$ kpc and $h_z = 0.25$ kpc.

Unfortunately this profile is not in galpy. So I tried fitting an exponential disk and a Miyamoto-Nagai disk to the particles. Results are shown in Figure 4 and 5[TO DO: I'm not sure, if I should use the total particle mass as total mass of the analytic disk, or leave it as a free parameter when fitting. But then I have to fit the profile to binned density.]

2. FIRST TESTS

2.1. *Fitting KKS-Pot*

3. CHANGES IN ROADMAPPING

3.1. *Outlier Model*

To exclude stars that are on weird orbits (e.g. moving with high radial velocity towards center of galaxy) and that are not covered by the assumed DF, we apply the following outlier model:

$$\begin{aligned} \mathscr{L}_i &\longrightarrow \max\left(\mathscr{L}_i, \epsilon \cdot \bar{\mathscr{L}}\right) \\ \mathscr{L}_i &= \text{likelihood of one single star given } p_M \\ \bar{\mathscr{L}} &= \text{median of all the } \mathscr{L}_i \\ \epsilon &= 0.001 \text{ for 20,000 stars} \end{aligned}$$

[TO DO: Should I take the median of $\mathscr{L}_i$ or $ln\mathscr{L}_i$?]

REFERENCES

D'Onghia, E., Vogelsberger, M., & Hernquist, L. 2013, ApJ, 766, 34

Springel, V., Di Matteo, T., & Hernquist, L. 2005, MNRAS, 361, 776

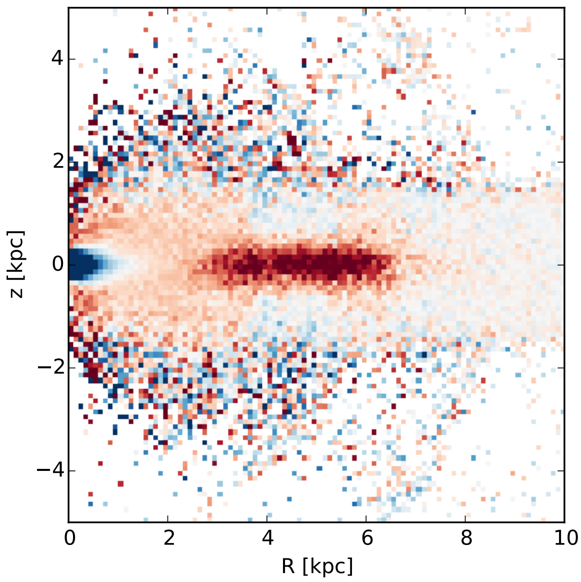

Figure 2. OBSOLET! Difference in average potential (keyword POT) per bin from particle types 2 and 3. This seems to be an effect of averaging over ϕ, see Figure 3.

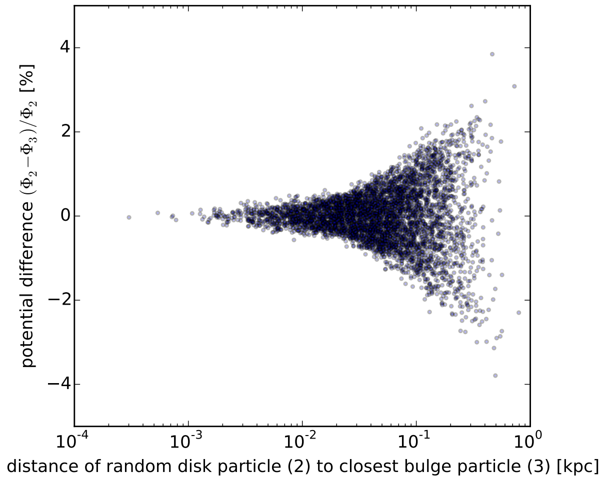

Figure 3. OBSOLET! Difference in POT keyword between a random type 2 particle and the type 3 particle that is closest. This demonstrates that particle types 2 and 3 measure the same quantity with their keyword POT.

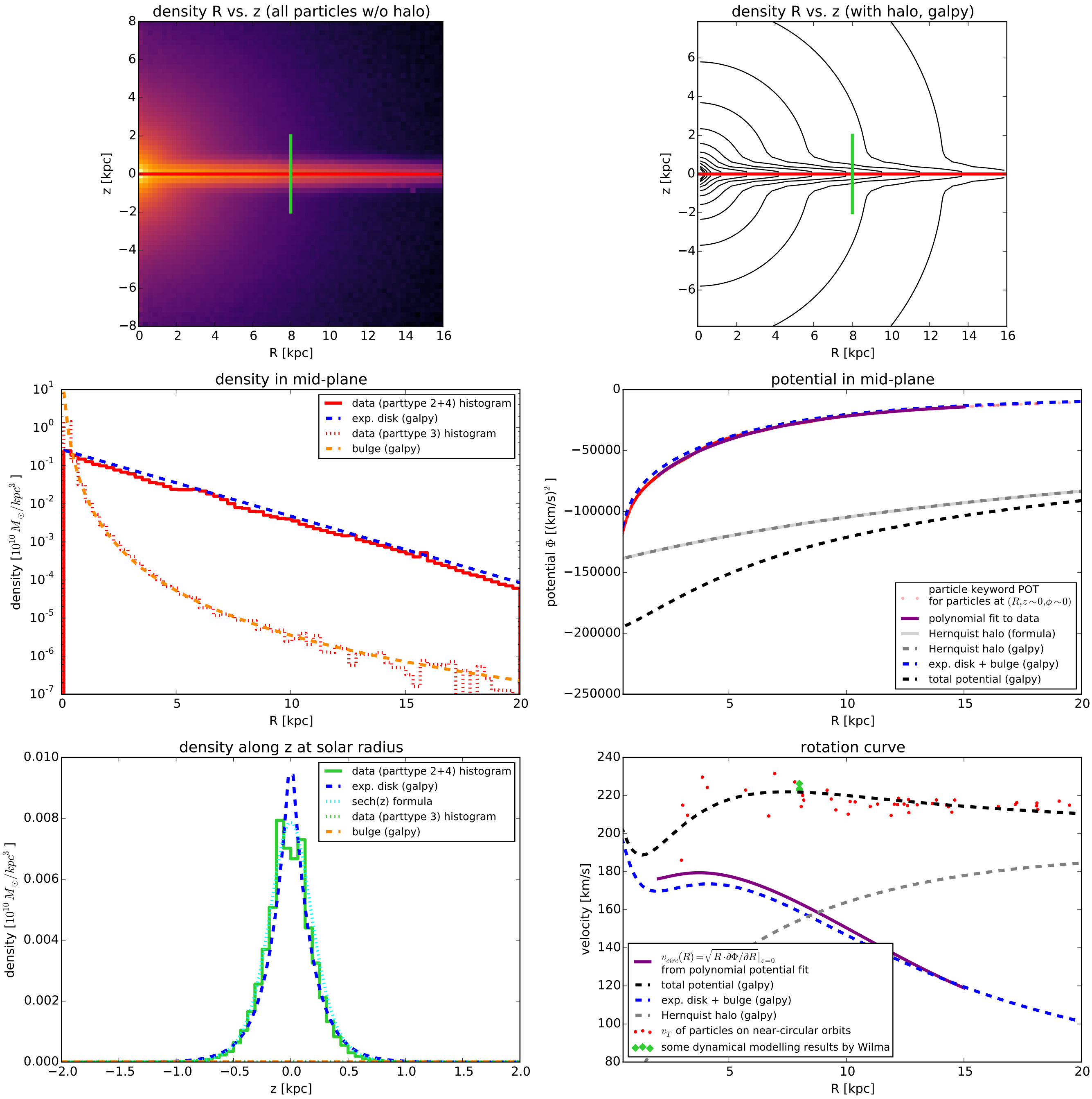

Figure 4. Comparing the simulation with the analytic functions for the disk, halo and bulge component in sections 1.5-1.7. I was using the DoubleExponentialDisk profile for the disk. Upper left: Density as derived from all simulation particles. Upper right: Contours of the galpy model density distribution. Middle left and bottom: Density along R at z=0 (red line) and z at $R_\odot$ (green line), comparing averaged simulation density profile for disk (solid) and bulge (dotted) and galpy model (dashed line) DoubleExponentialDisk (blue) and Hernquist bulge (orange). Middle right: Comparing the potential in the mid-plane from simulation keyword POT and the galpy model. From that it can be clearly seen that the keyword POT is the potential of the particles only. I cannot use it to figure out the dark matter halo. Upper right: Circular velocity curve.

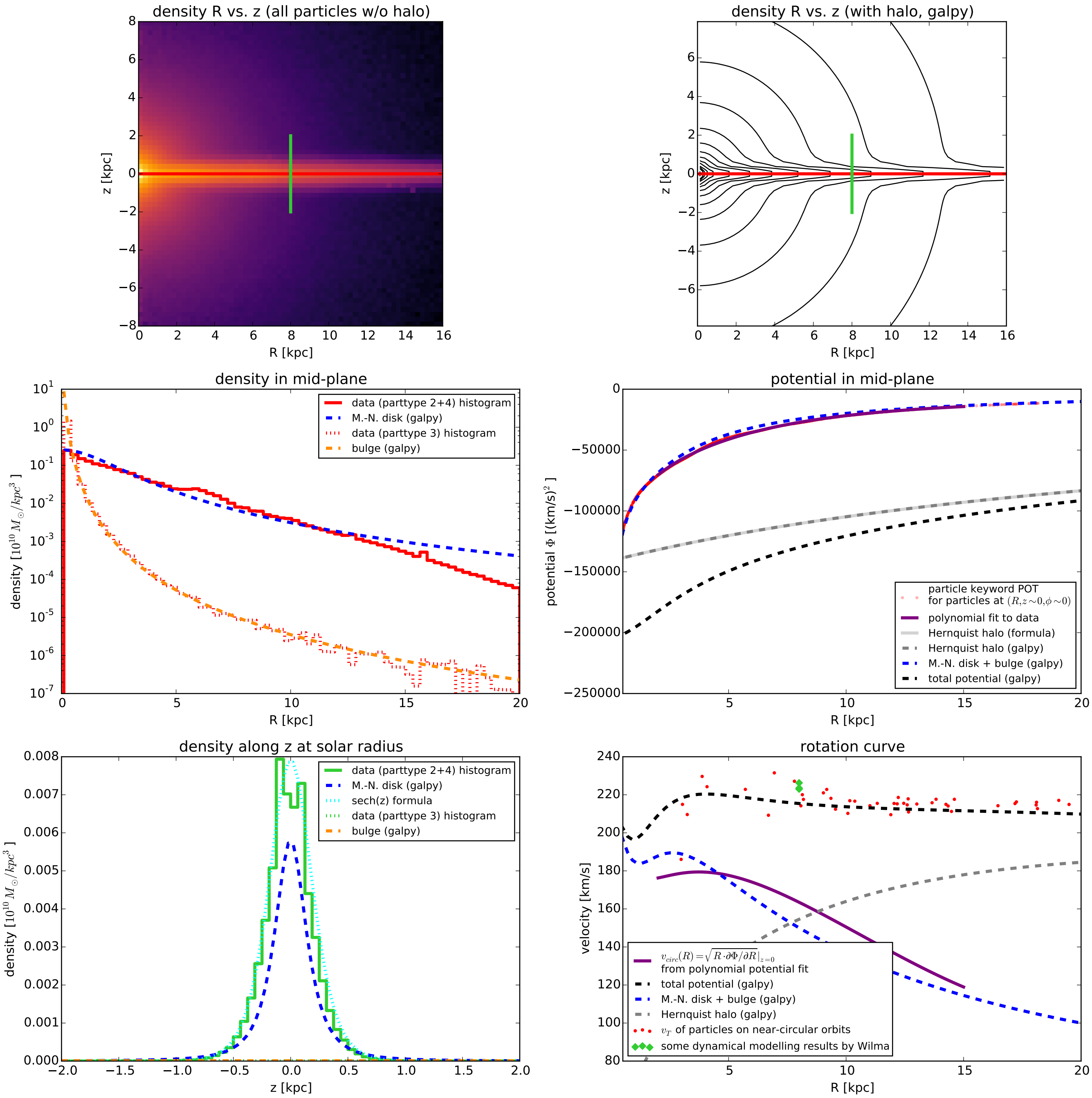

Figure 5. Same as Figure 4 but for a Miyamoto-Nagai disk instead of a DoubleExponentialDisk.

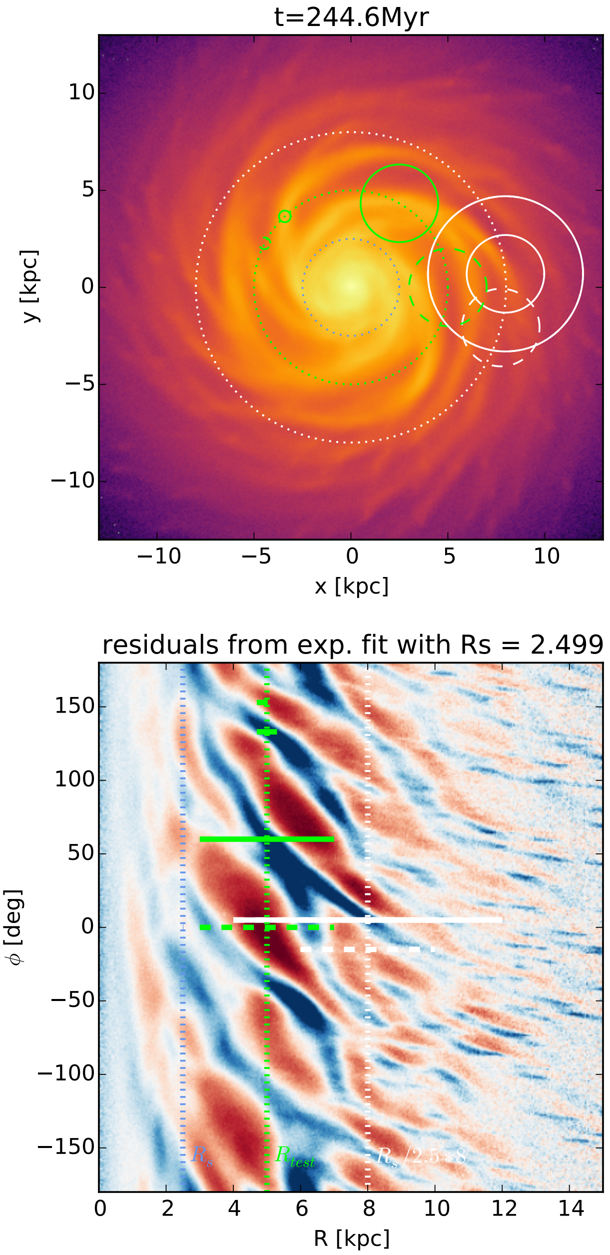

Figure 6. Observation volumes. Top: Density distribution of galaxy. Bottom: Residuals from exponential surface density fit with scale length 2.5 kpc. [TO DO: Calculate $\Sigma_{1.1\text{kpc}}$ for all observed voluminas and calcualte the contrast between those with spirals and those between spirals. We expect that for larger volumes the effect of spiral arms averages out and the difference should not be more than 10%-20% and therefore the modelling results are very similar to each other. In the small volume with $d_{max} = 300$ pc we however expect that the contrast is larger and therefore also modelling doesn't work as well.]

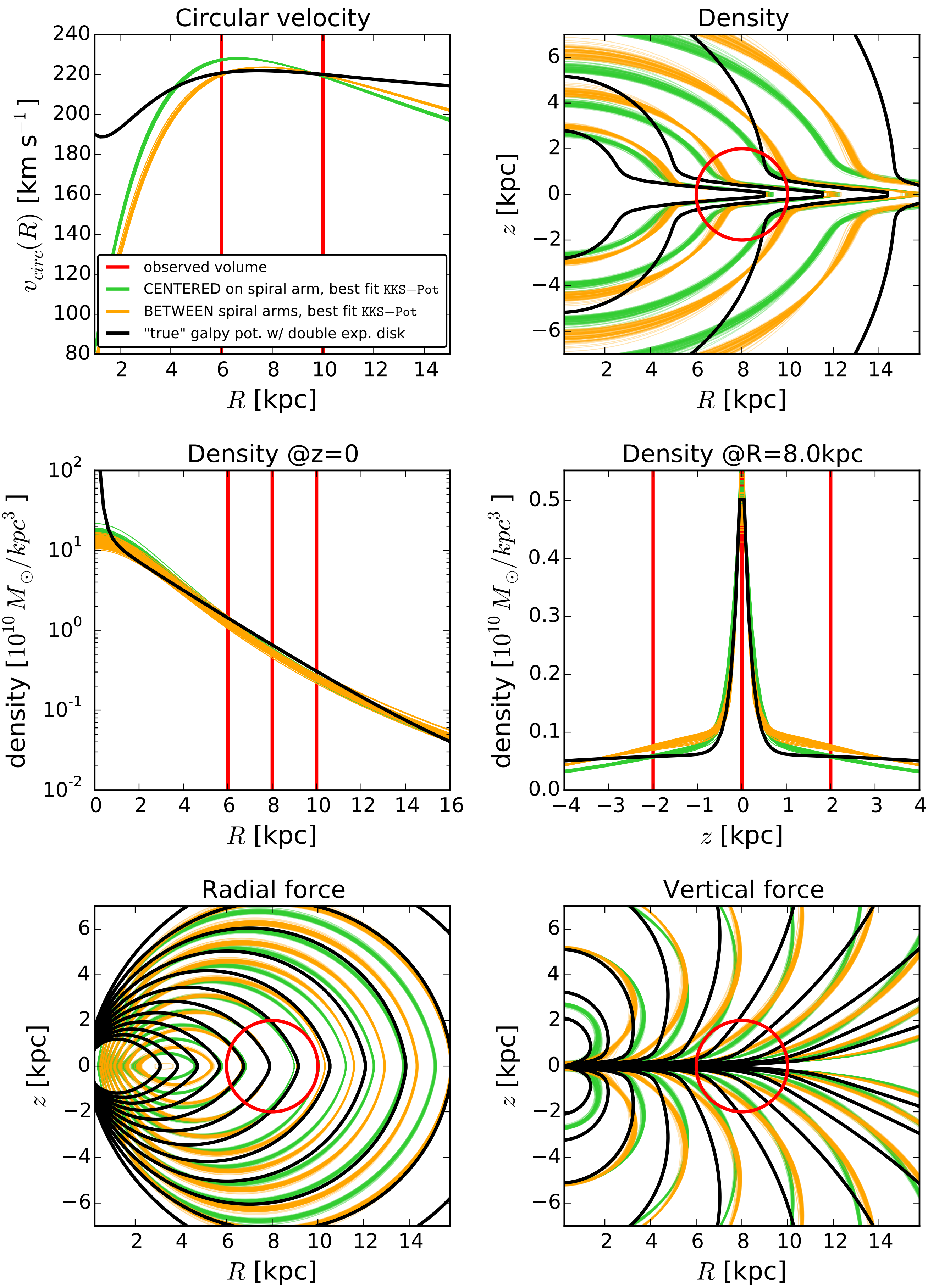

Figure 7. Potential deduced from the spheres with $d_{\max} = 2$ kpc around $R = 8$ kpc. Each 20,000 stars.

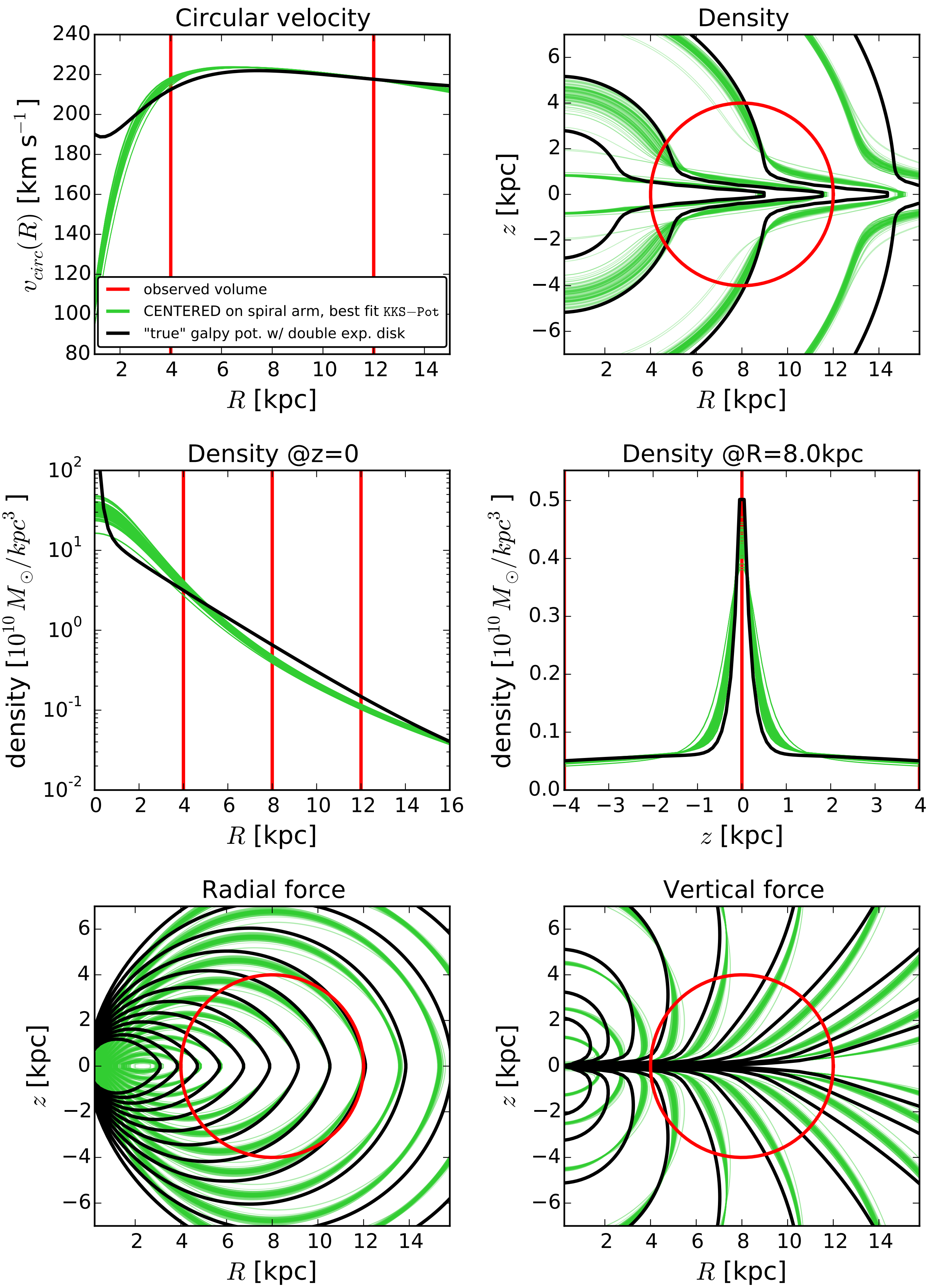

Figure 8. Potential deduced from the sphere with $d_{\max} = 4$ kpc around $R = 8$ kpc, centered on a spiral arm. Each 20,000 stars.

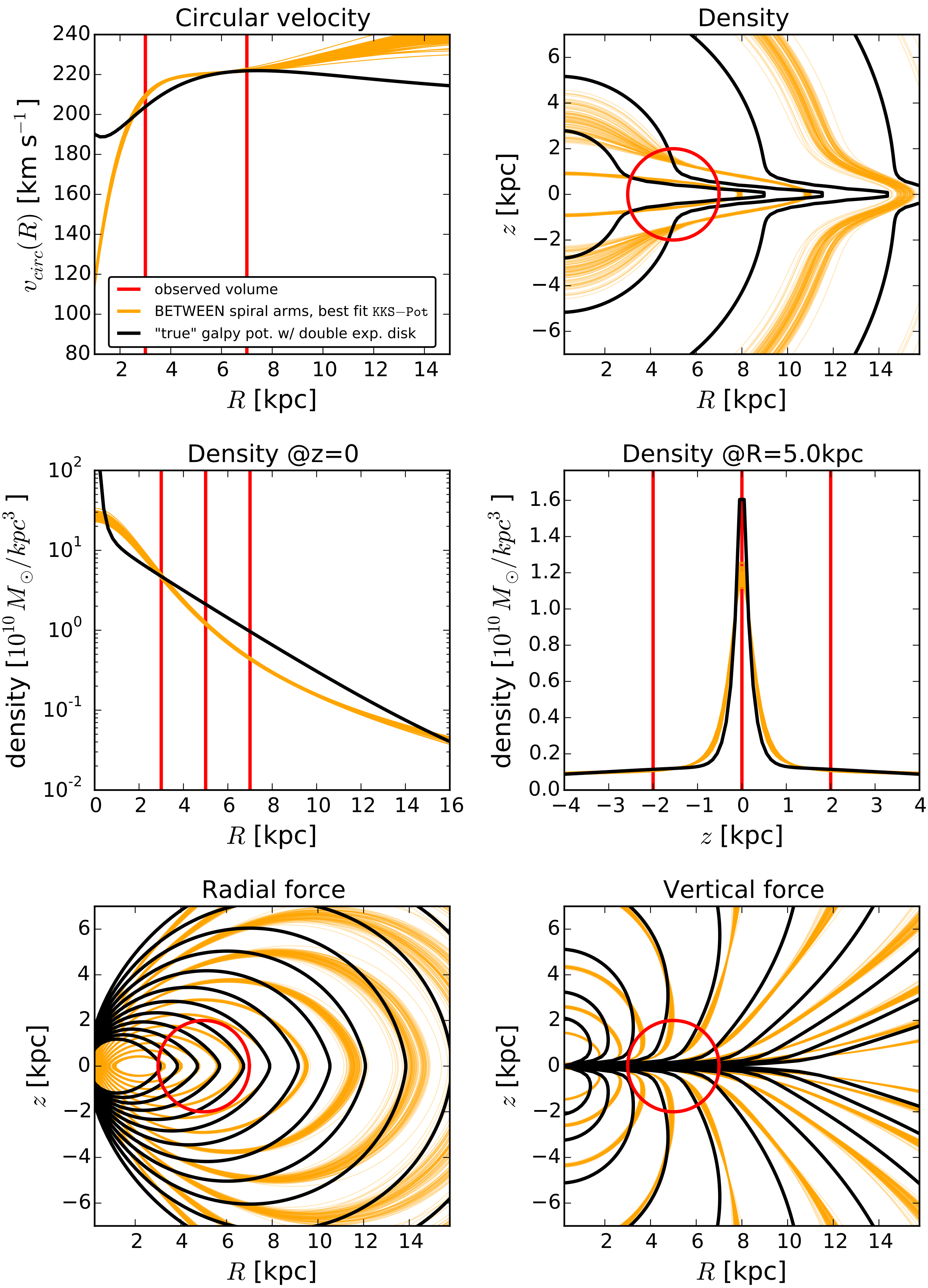

Figure 9. Potential deduced from the sphere with $d_{\max} = 2$ kpc around $R = 5$ kpc, centered between spiral arms. Each 20,000 stars.

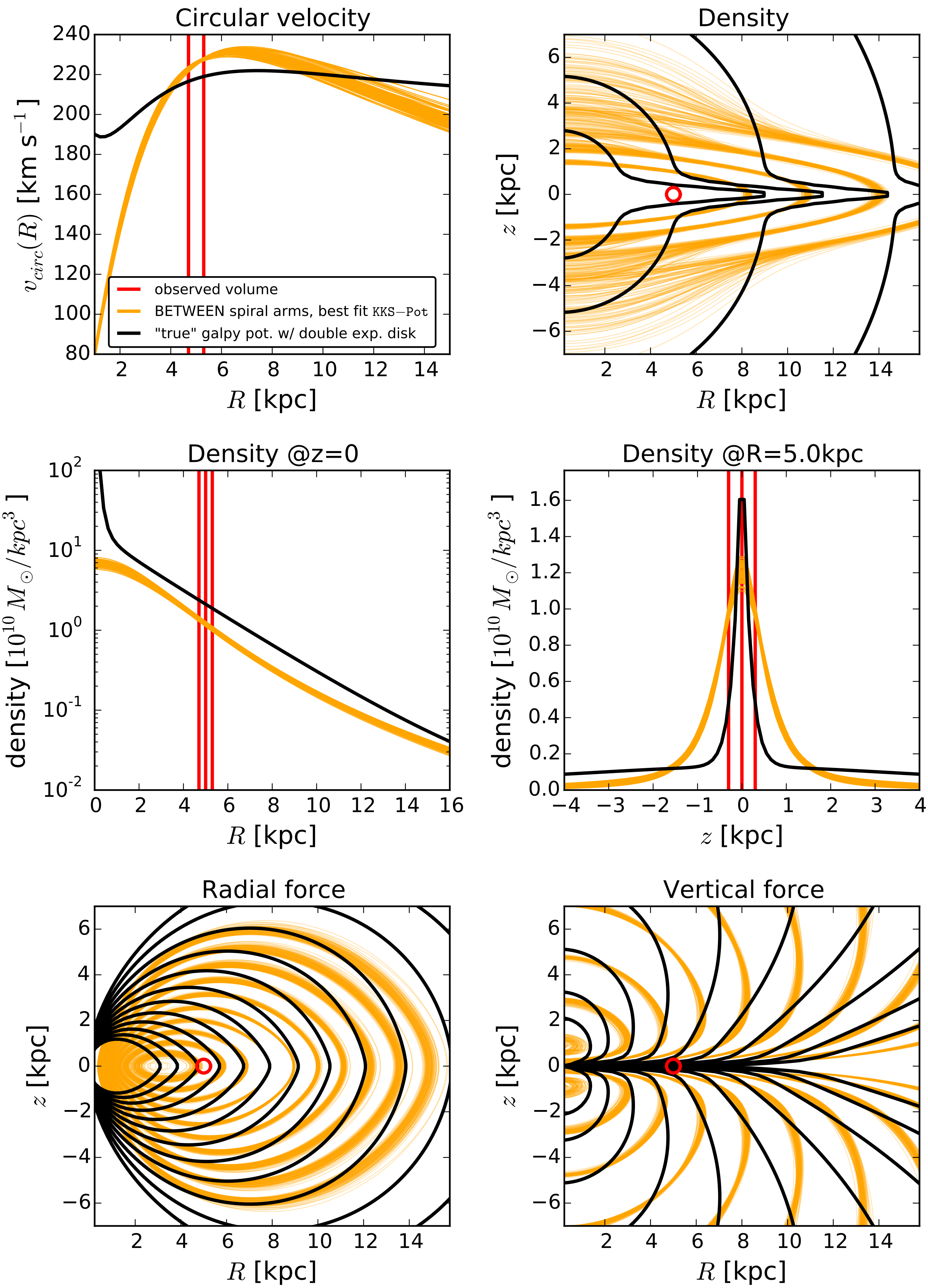

Figure 10. Potential deduced from the sphere with $d_{\max} = 300$ pc around $R = 5$ kpc, centered between spiral arms. Each 20,000 stars.

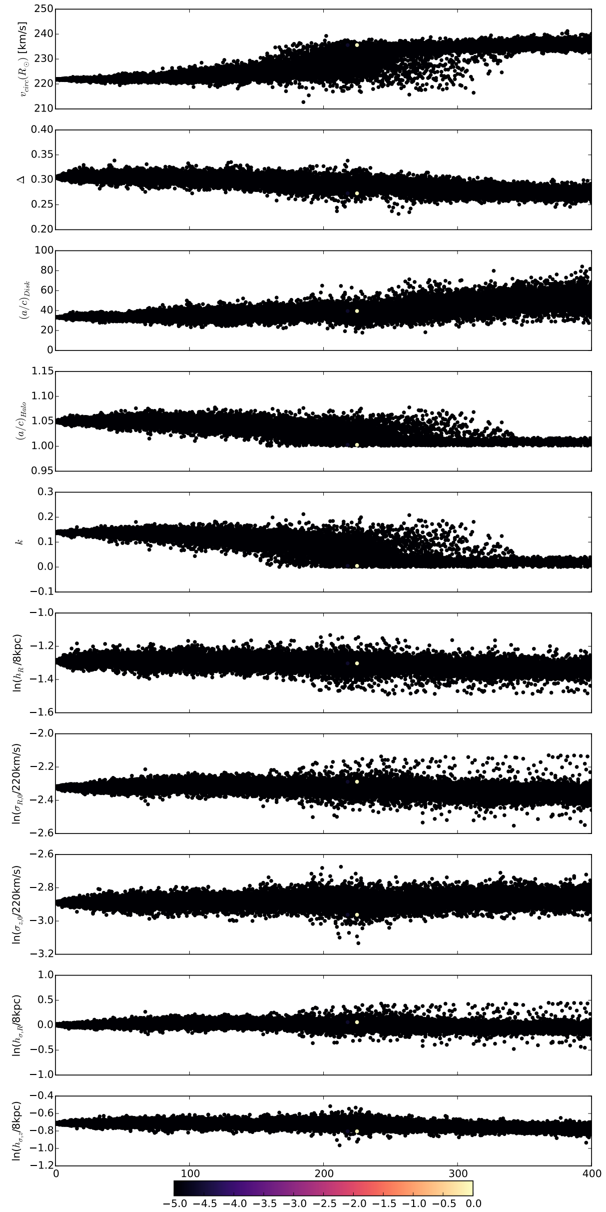

Figure 11. MCMC process for the sphere with $d_{\max} = 2$ kpc around $R = 5$ kpc, centered on a spiral arm, and fitting a KKS-Pot to it. Something is messed up as soon as the walkers fall down to $k = 0$ and $(a/c)_{halo} = 0$. [TO DO: Idea, what is going on here?]

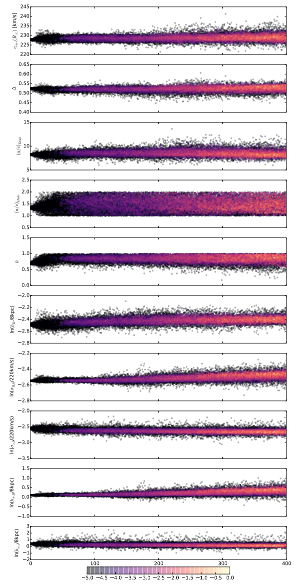

Figure 12. ... for the sphere with $d_{\max} = 0.3$ kpc around $R = 5$ kpc, centered between spiral arms, and fitting a KKS-Pot to it